

# On the Dimensionality of Wall and Target Return Subspaces in Through-the-Wall Radar Imaging

Zhihui Zhu and Michael B. Wakin

Department of Electrical Engineering and Computer Science  
Colorado School of Mines, Golden, CO, 80401, USA  
{zzhu,mwakin}@mines.edu

**Abstract**—Our objective is to detect and localize potential targets using stepped-frequency measurements consisting of both wall and target return from multiple antenna elements. We investigate the wall and target return subspaces both (i) for each antenna element separately and (ii) jointly for all antenna elements. Both the individual wall return subspace and the joint wall return subspace can capture most of the energy of the wall return, but the latter has much smaller dimensionality and thus captures less energy from the target return. Then, in each step of an iterative algorithm for detecting the target positions, we cancel the return from previously selected targets using a joint target return subspace model. The joint target return subspace offers improved target detection since this is better able to capture the return from a given target without capturing the energy of other targets.

**Keywords**—radar imaging, wall subspace, wall clutter mitigation, subspace projection, target subspace, target detection, Discrete Prolate Spheroidal Sequences

## I. INTRODUCTION

There are several approaches for mitigating wall return when detecting stationary targets through walls using stepped-frequency radar [1–5]. One approach involves modeling and subtracting wall return from the received data by estimating the parameters of the front wall [1]. A second approach uses spatial filtering to remove the direct current component corresponding to the wall return [2]. By estimating the wall return subspace via a singular value decomposition (SVD), Tivive et al. [3] mitigate wall clutter by projecting the full data onto the orthogonal complement of this subspace. A dictionary of multiband modulated Discrete Prolate Spheroidal Sequences (DPSS's) [6, 7] can also be utilized to efficiently represent the wall return for each antenna element separately [5, 8].

After the wall clutter is mitigated, the general approach for detecting sparse point targets is to first divide the target space in crossrange and downrange uniformly into a finite set of pixels. Then one constructs a dictionary of candidate return signatures based on these grid points and formulates the radar imaging problem as a sparse recovery problem [4, 5]. If a point target does not fall precisely on the grid, or in the more general case, if the target is not a point, then the return corresponding to the largest target reflectivity may dominate and sparse solvers may fail to detect the other targets. In order to detect and localize non-point targets, we recently [8, 9] proposed a DPSS-aided matching pursuit (MP) algorithm that uses a modulated DPSS basis to represent the target return separately at each antenna.

In this paper, we exploit the fact that since all antennas are observing the same wall and the same targets, jointly modeling the wall return across all antennas and jointly modeling the target return across all antennas yields subspace models with much smaller dimension than their counterparts [5, 8, 9] that arise with independent antenna-by-antenna modeling. The dimensionality of a target return subspace indicates the fundamental number of degrees of freedom in detecting that target and thus plays an important role in determining the number of measurements needed, for example, when applying compressive sensing (CS) techniques [10] to decrease the data size [4, 5, 8]. Our approach for characterizing the wall return subspace differs from [3] in that it is data-independent and thus can be efficiently utilized in CS problems [5, 8], whereas the [3] requires full data. We demonstrate the advantage of jointly considering the wall returns or the target returns both theoretically and experimentally. To be clear, throughout the paper, the term “jointly” refers to modeling (the wall return or the target return) across the antenna elements; we are not considering the wall and target returns together.

The outline of this paper is as follows. The main problem is illustrated in Section II. Section III investigates the dimensionality of the wall return subspace and the mitigation of wall clutter. Section IV discusses the dimensionality of the target return subspace and presents a new algorithm for detecting non-point targets. Section V presents simulations to support our proposed methods.

## II. PROBLEM SETUP

We consider an  $M$ -element synthetic linear aperture that transmits waveforms and receives the reflected signals. We assume that each transceiver transmits and receives a stepped-frequency signal consisting of  $N$  frequencies equispaced over the band  $[f_0, f_{N-1}]$  with the frequency step size  $\Delta F := \frac{f_{N-1} - f_0}{N-1}$ , i.e.,  $f_n = f_0 + n\Delta F$ . Further, we assume monostatic operation in which the transmitter and receiver are collocated as viewed from the target (i.e., the same antenna is used to transmit and receive) and after the antenna obtains the measurements in one location, we move it to the next location. To simplify the notation, we suppose the antennas are parallel to the wall. According to [5], we can model the wall return at the  $m$ -th antenna and the  $n$ -th frequency as

$$\mathbf{r}_m^w[n] := \sum_{l=0}^L \vartheta_l e^{-j2\pi f_n t_l}, \quad \forall m \in [M], n \in [N]. \quad (1)$$

Here,  $[N]$  denotes the set  $\{0, 1, \dots, N-1\}$  for any natural number  $N \in \mathbb{N}$ ;  $\vartheta_0$  is the complex reflectivity of the wall;  $\vartheta_l$ ,  $l \geq 1$  represents the complex reflectivity corresponding to the  $l$ -th wall reverberation and decreases with  $l$ ;  $L$  denotes the number of wall reverberations;  $t_0$  is the direct two-way travel time between the wall and the antenna; and  $t_l$ ,  $l \geq 1$  is the delay associated with the  $l$ -th wall return to the antenna.

Suppose there are  $K$  targets behind the wall. The target return observed by the  $m$ -th antenna at the  $n$ -th frequency can be expressed as

$$\mathbf{r}_m^t[n] := \sum_{k=1}^K \mathbf{r}_{k,m}^t[n], \quad (2)$$

where  $\mathbf{r}_{k,m}^t[n] := \int_{\tau_{k,m}^{\min}}^{\tau_{k,m}^{\max}} \sigma_k(\tau) e^{-j2\pi f_n \tau} d\tau$ . Here,  $\sigma_k(\tau)$  is the complex reflectivity function of the  $k$ -th target (we assume the target reflectivity is independent of frequency), and  $\tau_{k,m}^{\min}$  and  $\tau_{k,m}^{\max}$  are the minimum and maximum two-way travel times between the  $k$ -th target and the  $m$ -th antenna, respectively. Note that the return from point targets degenerates to  $\mathbf{r}_m^t[n] = \sum_{k=1}^K \sigma_k e^{-j2\pi f_n \tau_{k,m}}$ , where  $\tau_{k,m}$  is the two-way travel time between the  $k$ -th point target and the  $m$ -th antenna [5].

The measurement  $\mathbf{y}_m := \mathbf{r}_m^w + \mathbf{r}_m^t$  received by  $m$ -th antenna consists both wall and target return. Define  $\mathbf{r}^w = [(\mathbf{r}_0^w)^H \dots (\mathbf{r}_{M-1}^w)^H]^H$  and  $\mathbf{r}^t = [(\mathbf{r}_0^t)^H \dots (\mathbf{r}_{M-1}^t)^H]^H$ . Here  $H$  represents the conjugate transpose. The measurements  $\{\mathbf{y}_m\}_{m \in [M]}$  are arranged into an  $MN \times 1$  vector  $\mathbf{y} = \mathbf{r}^w + \mathbf{r}^t$ . From the measurements  $\mathbf{y}$ , our goal is to detect or localize the potential targets.

### III. WALL RETURN SUBSPACE

#### A. A bandpass modulated DPSS basis

Given  $W \in (0, \frac{1}{2})$ , the DPSS vectors  $\{\mathbf{s}_{N,W}^{(\kappa)}\}_{\kappa \in [N]}$  are length- $N$  vectors whose Discrete-Time Fourier Transform have a certain concentration in the digital frequency band  $[-W, W]$  [6, 7]. Define

$$\mathbf{e}_f := [e^{j2\pi f_0} e^{j2\pi f_1} \dots e^{j2\pi f_{(N-1)}}]^T \in \mathbb{C}^N$$

for all  $f \in \mathbb{R}$  as the sampled exponentials, where  $T$  represents the transpose operator. Let  $\mathbf{E}_{f_c} := \text{diag}(\mathbf{e}_{f_c})$  denote an  $N \times N$  diagonal matrix for any  $f_c \in \mathbb{R}$ . Define  $\mathbf{S}_{N,W} := [\mathbf{s}_{N,W}^{(0)} \mathbf{s}_{N,W}^{(1)} \dots \mathbf{s}_{N,W}^{(N-1)}]$ . Now define  $\mathbf{Q} := [\mathbf{E}_{f_c} \mathbf{S}_{N,W}]_J$  to be the first  $J$  modulated DPSS vectors for some value of  $J \in \{1, 2, \dots, N\}$  that we can choose as desired. The columns of  $\mathbf{Q}$  are orthonormal. For any matrix  $\mathbf{Q}$  with orthonormal columns, throughout the paper we use  $\mathbf{P}_{\mathbf{Q}} := \mathbf{I}_N - \mathbf{Q}\mathbf{Q}^H$  to denote an orthogonal projection from  $\mathbb{C}^N$  to the *orthogonal complement* of the subspace formed by the columns of  $\mathbf{Q}$ . Taking  $J \approx 2NW$ , the dictionary  $\mathbf{Q}$  provides very accurate approximations (in an MSE sense) for finite-length sample vectors arising from sampling random bandpass signals [7]. In fact, as stated below, all sampled sinusoids in the targeted band can be represented well by the dictionary  $\mathbf{Q}$ .

**Theorem III.1.** [11] Fix  $W \in (0, \frac{1}{2})$  and  $f_c \in \mathbb{R}$ . Define  $\mathbf{Q} := [\mathbf{E}_{f_c} \mathbf{S}_{N,W}]_J$ . For fixed  $\epsilon \in (0, 1)$ , choose  $J = 2NW(1 + \epsilon)$ . Then there exist constants  $C_1, C_2$  (where  $C_1, C_2$  may depend on  $W$  and  $\epsilon$ ) such that for all  $N \geq N_0$

$$\|\mathbf{P}_{\mathbf{Q}} \mathbf{e}_f\|_2 \leq C_1 N^{5/4} e^{-C_2 N}, \quad \forall f \in [f_c - W, f_c + W].$$

In a nutshell, this result states that (i) the effective dimensionality of the subspace spanned by  $\{\mathbf{e}_f\}_{f \in [f_c - W, f_c + W]}$  is  $2NW$ , and (ii) the modulated DPSS vectors provide a basis for this subspace.

#### B. The dimensionality of the wall return subspace

If we consider only the direct wall return, the wall return defined in (1) reduces to

$$\mathbf{r}_m^w[n] = \vartheta_0 e^{-j2\pi f_n t_0} = \vartheta_0 e^{-j2\pi f_0 t_0} e^{-j2\pi n \Delta F t_0}.$$

In this simple case, the wall return  $\mathbf{r}_m^w$  lives in a 1-dimensional subspace spanned by the basis vector  $\mathbf{e}_{-\Delta F t_0}$ .

More generally, the wall return in (1) can be rewritten as

$$\mathbf{r}_m^w[n] = \sum_{l=0}^L \vartheta_l e^{-j2\pi f_0 t_l} e^{-j2\pi n t_l \Delta F}. \quad (3)$$

From Theorem III.1, we expect that the wall return  $\mathbf{r}_m^w$  at one antenna will approximately live within a low-dimensional subspace because (3) indicates that  $\mathbf{r}_m^w$  can be viewed as a linear combination of sampled exponentials  $\mathbf{e}_f$  with  $f \in [-t_L \Delta F, -t_0 \Delta F]$ . Accordingly, define the dictionary of modulated DPSS vectors

$$\mathbf{D}_m := [\mathbf{E}_{-\Delta F(t_L+t_0)/2} \mathbf{S}_{N, \Delta F(t_L-t_0)/2}]_{J^w}$$

for some value of  $J^w \in \{1, 2, \dots, N\}$ .

**Corollary III.2.** Fix  $\epsilon \in (0, 1)$ . Choose  $J^w = N(t_L - t_0)\Delta F(1 + \epsilon)$ . Then there exist constants  $C_1, C_2$  and an integer  $N_0$  such that for all  $N \geq N_0$

$$\|\mathbf{P}_{\mathbf{D}_m} \mathbf{r}_m^w\|_2 \leq \sum_{l=0}^L \vartheta_l C_1 N^{5/4} e^{-C_2 N}.$$

The proof follows directly from Theorem III.1. The above result indicates that  $\mathbf{r}_m^w$  is approximately within  $\mathbb{S}_{\mathbf{D}_m}$ , the column space of  $\mathbf{D}_m$  when we set  $J^w = N(t_L - t_0)\Delta F(1 + \epsilon)$ . Define the  $MN \times MJ^w$  block diagonal matrix  $\mathbf{D} := \text{diag}(\mathbf{D}_0, \dots, \mathbf{D}_{M-1})$ .

**Corollary III.3.** Fix  $\epsilon \in (0, 1)$ . Choose  $J^w = N(t_L - t_0)\Delta F(1 + \epsilon)$ . Then there exist constants  $C_1, C_2$  and an integer  $N_0$  such that for all  $N \geq N_0$

$$\|\mathbf{P}_{\mathbf{D}} \mathbf{r}^w\|_2 \leq M \sum_{l=0}^L \vartheta_l C_1 N^{5/4} e^{-C_2 N}.$$

In words, the complete wall return  $\mathbf{r}^w$  lives approximately within  $\mathbb{S}_{\mathbf{D}}$ , the subspace spanned by the columns of  $\mathbf{D}$ . The dimension of  $\mathbb{S}_{\mathbf{D}}$  is  $MJ^w$ .

Before moving on, we note that the electrical properties of the wall material, which directly determine  $\{t_l\}_{l=1}^L$ , may not be known in advance. The dictionary  $\mathbf{D}_m$  cannot capture the wall return completely if  $t_L$  is chosen too small. On the other hand, choosing  $t_L$  too large may result in a dictionary  $\mathbf{D}_m$  that also captures some energy from target returns behind the wall. Since simulations have indicated that almost all walls have dominant reverberations up to 1.5m behind the wall [5], we use the same strategy as [5] in that we mitigate the wall reverberations up to 1.5m behind the wall. Note that we can still detect some targets located less than 1.5m behind the wall

as long as there exist some antennas that have distance larger than 1.5m from these targets.

Because we assume the antennas are parallel to the wall, the wall return  $\mathbf{r}_m^w$  is identical for different  $m$ . Therefore, the wall return  $\mathbf{r}^w$  actually lives within a subspace which has much smaller dimension than  $\mathbb{S}_D$ . Define  $\hat{D} := \frac{1}{\sqrt{M}}[D_0^H D_1^H \dots D_{M-1}^H]^H$ .

**Corollary III.4.** Fix  $\epsilon \in (0, 1)$ . Choose  $J^w = N(t_L - t_0)\Delta F(1+\epsilon)$ . Then there exist constants  $C_1, C_2$  and an integer  $N_0$  such that for all  $N \geq N_0$

$$\|P_{\hat{D}}\mathbf{r}^w\|_2 \leq M \sum_{l=0}^L \vartheta_l C_1 N^{5/4} e^{-C_2 N}.$$

We omit the proof due to limited space. The dimension of  $\mathbb{S}_{\hat{D}}$  (the column space of  $\hat{D}$ ) is  $J^w$ , which is smaller than the dimension of  $\mathbb{S}_D$  by a factor of  $M$ . The advantage of this smaller dimension is that the projection operator  $P_{\hat{D}}$  has less effect on the target return  $\mathbf{r}^t$  than  $P_D$ . We give an example to illustrate this. We simulate one line target of length 0.5m located at  $(x, y) = (-0.29\text{m}, 5.38\text{m})$ , with complex reflectivity of 5. An  $M = 15$ -element synthetic linear aperture (located along the  $x$ -axis) with interelement spacing of  $\frac{4}{M}$ m is used. A stepped-frequency signal consisting of  $N = 101$  frequencies from 1GHz to 3GHz is utilized to obtain measurements. A front wall is located at  $y = 3.13\text{m}$ , i.e., 3.13m away from the antennas.

We generate target return according to (2). On the basis of (1),  $L = 5$  wall reverberations are generated equally spaced between the wall and 1.5m behind the wall with  $\vartheta_0 = 30$  and  $\vartheta_l = \frac{1}{1+l}\vartheta_0$  for all  $l = 1, \dots, L$ . We have  $N(t_L - t_0)\Delta F = 20.2 \approx 20$ . Figures 1(a-b) respectively show the ability of  $D$  (and  $\hat{D}$ ) to capture the energy in the wall return  $\mathbf{r}^w$  through the quantification  $\text{SNR}_1 = 20 \log_{10}(\frac{\|\mathbf{r}^w\|_2}{\|P_D\mathbf{r}^w\|_2})$  dB and avoid the target return  $\mathbf{r}^t$  through the quantification  $\text{SNR}_2 = 20 \log_{10}(\frac{\|\mathbf{r}^t\|_2}{\|\mathbf{r}^t - P_D\mathbf{r}^t\|_2})$  with various  $J^w$  near 20. As can be observed, though  $D$  and  $\hat{D}$  capture the same energy in the wall return,  $\hat{D}$  captures less energy in the target return.

Also, as anticipated, both  $D$  and  $\hat{D}$  may capture non-negligible energy from the target return if we choose  $J^w$  too large, whereas choosing  $J^w$  too small results in a dictionary that cannot capture the wall return completely. There is a tradeoff between cancelling the wall return and preserving the target return. By changing  $J^w$ , we can balance this tradeoff. In general  $J^w \approx N(t_L - t_0)\Delta F$  is recommended for most applications.

### C. Wall clutter mitigation

Based on the discussion above, one could mitigate wall clutter antenna-by-antenna by computing [8]

$$\tilde{\mathbf{y}}_m := P_{D_m}\mathbf{y}_m = P_{D_m}\mathbf{r}_m^w + P_{D_m}\mathbf{r}_m^t.$$

Since  $P_{D_m}\mathbf{r}_m^w \approx 0$ , we get  $\tilde{\mathbf{y}}_m \approx P_{D_m}\mathbf{r}_m^t$ . The processed measurements could then be written as

$$\tilde{\mathbf{y}} = P_D\mathbf{y} = P_D\mathbf{r}^w + P_D\mathbf{r}^t \approx P_D\mathbf{r}^t.$$

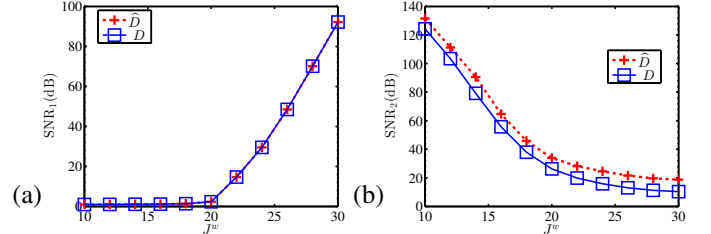


Fig. 1. (a)  $\text{SNR}_1$  captured for wall return as a function of  $J^w$ ; (b)  $\text{SNR}_2$  captured for target return as a function of  $J^w$ .

Alternatively, one could mitigate the wall clutter jointly by computing

$$\hat{\mathbf{y}} = P_{\hat{D}}\mathbf{y} = P_{\hat{D}}\mathbf{r}^w + P_{\hat{D}}\mathbf{r}^t \approx P_D\mathbf{r}^t.$$

Since  $P_{\hat{D}}$  has less effect on the target return  $\mathbf{r}^t$  than  $P_D$ , we adopt  $P_{\hat{D}}$  for mitigating the wall return.

## IV. TARGET RETURN SUBSPACE

### A. The dimensionality of target return subspaces

The target return observed by the  $m$ -th antenna corresponding to the  $k$ -th target can be rewritten as  $\mathbf{r}_{k,m}^t[n] = \int_{\tau_{k,m}^{\min}}^{\tau_{k,m}^{\max}} \sigma_k(\tau) e^{-j2\pi f_0 \tau} e^{-j2\pi n \tau \Delta F} d\tau$ . This indicates that  $\mathbf{r}_{k,m}^t$  can be viewed as a linear combination of sampled exponentials  $e_f$  with  $f \in [-\tau_{k,m}^{\max} \Delta F, -\tau_{k,m}^{\min} \Delta F]$ . Thus, from Theorem III.1, we expect this vector to approximately live within a low-dimensional subspace spanned by certain modulated DPSS vectors. Define

$$\Psi_{k,m} := [\mathbf{E}_{-\Delta F(\tau_{k,m}^{\min} + \tau_{k,m}^{\max})/2} \mathbf{S}_{N, \Delta F(\tau_{k,m}^{\max} - \tau_{k,m}^{\min})/2}] J_{k,m}^t$$

for some value of  $J_{k,m}^t \in \{1, 2, \dots, N\}$ .

**Theorem IV.1.** [11] Fix  $\epsilon \in (0, 1)$ . Choose  $J_{k,m}^t = N(\tau_{k,m}^{\max} - \tau_{k,m}^{\min})\Delta F(1+\epsilon)$ . Then there exist constants  $C_1, C_2$  and an integer  $N_0$  such that for all  $N \geq N_0$

$$\|P_{\Psi_{k,m}}\mathbf{r}_{k,m}^t\|_2 \leq \sqrt{\int_{\tau_{k,m}^{\min}}^{\tau_{k,m}^{\max}} \sigma_k^2(\tau) d\tau} C_1 N^{5/4} e^{-C_2 N}.$$

The above result indicates that  $\mathbf{r}_{k,m}^t$  is approximately contained within the column space of  $\Psi_{k,m}$ . Define

$$\Psi_k := \text{diag}(\Psi_{0,k}, \dots, \Psi_{M-1,k}). \quad (4)$$

Let  $\bar{\mathbf{r}}_k^t := [(\mathbf{r}_{k,0}^t)^H \dots (\mathbf{r}_{k,M-1}^t)^H]^H$  denote the joint target return (across all antennas) corresponding to the  $k$ -th target.

**Corollary IV.2.** Fix  $\epsilon \in (0, 1)$ . Choose  $J_{k,m}^t = N(\tau_{k,m}^{\max} - \tau_{k,m}^{\min})\Delta F(1+\epsilon)$ . Then there exist constants  $C_1, C_2$  and an integer  $N_0$  such that for all  $N \geq N_0$

$$\|P_{\Psi_k}\bar{\mathbf{r}}_k^t\|_2 \leq \sum_{m=0}^{M-1} \sqrt{\int_{\tau_{k,m}^{\min}}^{\tau_{k,m}^{\max}} \sigma_k^2(\tau) d\tau} C_1 N^{5/4} e^{-C_2 N}.$$

This result follows directly from Theorem IV.1. In words, the target return  $\bar{\mathbf{r}}_k^t$  lives approximately within  $\mathbb{S}_{\Psi_k}$ , the subspace spanned by the columns of  $\Psi_k$ . The dimension of  $\mathbb{S}_{\Psi_k}$  is  $J_k^t := \sum_{m=0}^{M-1} J_{k,m}^t$ .

Now, similar to the case of the wall return, if we utilize the fact that  $\{\mathbf{r}_{k,m}^t\}_m$  correspond to the same target, we expect

that the joint target return  $\bar{\mathbf{r}}_k^t$  can be captured using a subspace with dimension much smaller than  $\mathbb{S}_{\Psi_k}$ . Divide the  $k$ -th target uniformly into  $P$  points and construct  $\mathbf{G}_{k,m} \in \mathbb{C}^{N \times P}$  with entries given by

$$\mathbf{G}_{k,m}[n,p] := e^{-j2\pi f_n \tau_{p,m}} \quad (5)$$

for  $n \in [N]$  and  $p \in [P]$ . Here  $\tau_{p,m}$  denotes the two-way travel time between the  $p$ -th point position and the  $m$ -th transceiver. One can approximate  $\mathbf{r}_{k,m}^t$  as a linear combination of the columns of  $\mathbf{G}_{k,m}$ . In fact, an approximate method to generate the modulated DPSS basis  $\Psi_{k,m}$  (whose columns are also the eigenvectors of the covariance matrix of a randomly chosen sinusoid in the frequency band of interest, see [7]) is by computing the left singular vectors of  $\mathbf{G}_{k,m}$ .

Choosing  $P$  sufficiently large, the matrix  $\mathbf{G}_{k,m}$  is approximately low rank with effective rank  $\approx N(\tau_{k,m}^{\max} - \tau_{k,m}^{\min})\Delta F$ . Arrange  $\{\mathbf{G}_{k,m}\}_{m \in [M]}$  as

$$\mathbf{G}_k := [\mathbf{G}_{k,0}^H \ \mathbf{G}_{k,1}^H \ \cdots \ \mathbf{G}_{k,M-1}^H]^H. \quad (6)$$

Now, one can approximate  $\bar{\mathbf{r}}_k^t$  as a linear combination of the columns of  $\mathbf{G}_{k,m}$ . The effective rank of  $\mathbf{G}_k$  is upper bounded by  $\approx \sum_{m=0}^{M-1} N(\tau_{k,m}^{\max} - \tau_{k,m}^{\min})\Delta F$  and lower bounded by  $\max_m N(\tau_{k,m}^{\max} - \tau_{k,m}^{\min})\Delta F$ . We use an example to illustrate the low rank structure in both  $\mathbf{G}_{k,m}$  and  $\mathbf{G}_k$ . With the same setup to that in Section III-B, we set  $P = 50$ . Figures 2(a-b) display the singular values of  $\mathbf{G}_{1,0}$  and  $\mathbf{G}_1$ , respectively. We observe that the effective rank of  $\mathbf{G}_1$  is only slightly larger than  $\mathbf{G}_{1,0}$ . Here  $N(\tau_{1,0}^{\max} - \tau_{1,0}^{\min})\Delta F = 2.04 \approx 2$ . Although not shown in the plot, we also note that the effective ranks of  $\mathbf{G}_{k,m}$  and  $\mathbf{G}_k$  both scale proportionally with the size of the target.

Let  $\mathbf{G}_{k,m} = \mathbf{U}_{k,m} \Sigma_{k,m} \mathbf{V}_{k,m}^H$  be an SVD of  $\mathbf{G}_{k,m}$ , where  $\Sigma_{k,m}$  is a diagonal matrix with singular values  $\gamma_{k,m}^{(p)}$  (which are arranged in non-increasing order, i.e.,  $\gamma_{k,m}^{(0)} \geq \gamma_{k,m}^{(1)} \geq \cdots$ ) along its diagonal. For given  $0 < \beta < 1$ , define  $\bar{J}_{k,m}^t$  as the number of singular values that are greater than  $\beta \gamma_{k,m}^{(0)}$ , i.e.,  $\bar{J}_{k,m}^t := \#\{p, \gamma_{k,m}^{(p)} \geq \beta \gamma_{k,m}^{(0)}\}$ . Define  $\bar{J}_k^t := \sum_{m=0}^{M-1} \bar{J}_{k,m}^t$ . Similarly, let  $\mathbf{G}_k = \mathbf{U}_k \Sigma_k \mathbf{V}_k^H$  be an SVD of  $\mathbf{G}_k$ , where  $\Sigma_k$  is a diagonal matrix with singular values  $\gamma_k^{(p)}$  (which are arranged in non-increasing order) along its diagonal. Let  $\hat{J}_k^t$  denote the number of singular values that are greater than  $\beta \gamma_k^{(0)}$ . Define

$$\begin{aligned} \bar{\Psi}_k &:= \text{diag}([\mathbf{U}_{k,0}]_{\bar{J}_{k,0}^t} \ \cdots \ [\mathbf{U}_{k,M-1}]_{\bar{J}_{k,M-1}^t}), \\ \hat{\Psi}_k &:= [\mathbf{U}_k]_{\hat{J}_k^t}, \end{aligned}$$

where  $[\mathbf{U}_{k,m}]_{\bar{J}_{k,m}^t}$  is obtained by taking the first  $\bar{J}_{k,m}^t$  columns of  $\mathbf{U}_{k,m}$ . Similar notation holds for  $[\mathbf{U}_k]_{\hat{J}_k^t}$ .

We add one more line target of length 0.5m located at (1.55m, 6.38m), with relative complex reflectivity of 3. Figure 2(c) shows  $J_1^t$ ,  $\bar{J}_1^t$  and  $\hat{J}_1^t$  for various  $\beta$ . Here set  $J_{k,m}^t = \bar{J}_{k,m}^t$  and thus  $J_1^t = \bar{J}_1^t$ . We observe that the effective dimensionality of the first target return subspace is much smaller when we consider the antennas jointly. Figures 2(d-e) respectively show the ability of  $\Psi_1$  (and  $\bar{\Psi}_1$ ,  $\hat{\Psi}_1$ ) to capture the energy in the first target return  $\bar{\mathbf{r}}_1^t$  through

the quantification  $\text{SNR}_1 = 20 \log_{10}(\frac{\|\bar{\mathbf{r}}_1^t\|_2}{\|\mathbf{P}_{\Psi_1} \bar{\mathbf{r}}_1^t\|_2})$  dB and to avoid the second target return  $\bar{\mathbf{r}}_2^t$  through the quantification  $\text{SNR}_2 = 20 \log_{10}(\frac{\|\bar{\mathbf{r}}_2^t\|_2}{\|\bar{\mathbf{r}}_2^t - \mathbf{P}_{\Psi_1} \bar{\mathbf{r}}_2^t\|_2})$  with various  $\beta$ . As can be seen,  $\Psi_1$ ,  $\bar{\Psi}_1$  and  $\hat{\Psi}_1$  have almost the same ability to represent the first target return  $\bar{\mathbf{r}}_1^t$ . However, compared to  $\Psi_1$  and  $\bar{\Psi}_1$ ,  $\hat{\Psi}_1$  captures less energy in the second target return  $\bar{\mathbf{r}}_2^t$ . This advantage owes to the fact that  $\hat{\Psi}_1$  has a much smaller number of columns.

## B. Target detection

Following the general approach for radar imaging [5], the target space is divided uniformly into a grid of  $L_x \times L_y$  pixels. We arrange the pixels of the image into an  $L_x L_y \times 1$  vector  $\alpha$ . Define  $\Theta_m \in \mathbb{C}^{N \times L_x L_y}$  with entries given by  $\Theta_m[n, q] := e^{-j2\pi f_n \tau_{q,m}}$  for  $n \in [N]$  and  $q \in [L_x L_y - 1]$ . Here  $\tau_{q,m}$  denotes the two-way travel time between the  $q$ -th grid and the  $m$ -th transceiver. The target return can be written as  $\mathbf{r}_m^t = \Theta_m \alpha$  if the targets are points and located precisely on the grid. Define  $\Theta := [\Theta_0^H \ \cdots \ \Theta_{M-1}^H]^H$ .

In order to detect and localize the non-point targets, we [8, 9] modify the iterative, greedy matching pursuit (MP) algorithm [12] so that the energy of exponentials with two-way traveling time close to that of each selected point is cancelled by using a modulated DPSS basis. To account for and cancel off-grid target return, for each  $q \in [L_x L_y - 1]$ , we generate  $\bar{\Psi}_q$  and  $\hat{\Psi}_q$  by uniformly dividing a region centered at grid point  $q$  with size  $R_x \times R_y$  m into  $F_x \times F_y$  points, constructing  $\mathbf{G}_{q,m}$  as defined in (5) with  $P = F_x F_y$ , constructing  $\mathbf{G}_q$  as defined in (6), and finally computing the left singular vectors of  $\mathbf{G}_{q,m}$  and  $\mathbf{G}_q$ . Throughout the simulations, we choose  $R_x = 1$ ,  $R_y = 0.3$ ,  $F_x = 12$  and  $F_y = 6$ .  $\Psi_q$  is also generated for this region according to (4). The full subspace-based MP algorithm for target detection is shown in Algorithm 1. As shown in the merge step, in each iteration when we pick one pixel in the grid, we also choose its neighbors (from two pixels to the left to two pixels to the right). We note that this step (adding its neighbors) is used only to improve the imaging result, but has no effect in detection. The size of the neighbors can be adapted to the particular application.

---

### Algorithm 1 Subspace-based Matching Pursuit.

---

**input:**  $\Theta$  with columns  $\theta_j$ ,  $\hat{\mathbf{y}}$ , number of iterations  $I$

**initialize:**  $\mathbf{r}^0 = \hat{\mathbf{y}}$ ,  $\hat{\alpha} = 0$ ,  $i = 0$ ,  $\Lambda^0 = \emptyset$

1: **while**  $i < I$  **do**

2: identify:  $j_0 = \arg \max_j |\theta_j^H \mathbf{r}^i| / \|\theta_j\|_2$

3: merge:  $\Lambda^{i+1} = \Lambda^i \cup \{j_0 - 2, j_0 - 1, j_0, j_0 + 1, j_0 + 2\}$

4: update:  $\mathbf{r}^{i+1} = \mathbf{P}_{\Psi_{j_0}} \mathbf{r}^i$  (or  $\mathbf{P}_{\bar{\Psi}_{j_0}} \mathbf{r}^i$ ,  $\mathbf{P}_{\hat{\Psi}_{j_0}} \mathbf{r}^i$ )  
 $i = i + 1$

5: **end while**

6: **return**  $\hat{\alpha} = \Theta_{\Lambda}^{\dagger} \hat{\mathbf{y}}$

---

## V. SIMULATIONS

With the same setup to that in Section III-B, we simulate eight line targets of length 0.5m as listed in Table I. The  $4\text{m} \times 5.5\text{m}$  region centered at (0m, 4.75m) is chosen to be imaged, and it is divided into a grid of  $33 \times 77$  pixels. The number  $J^w$

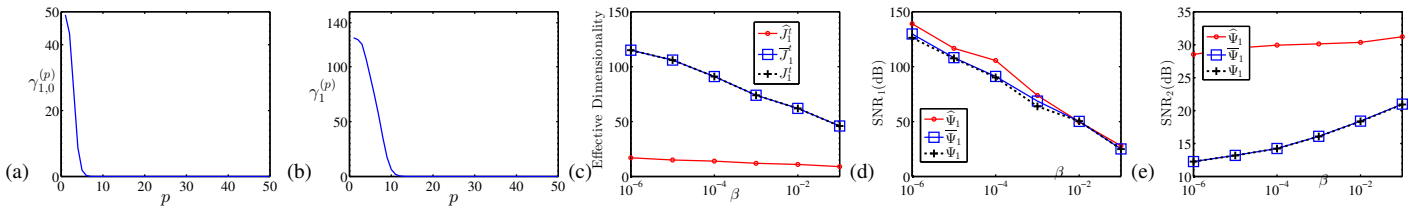


Fig. 2. (a) the singular values of  $\mathbf{G}_{1,0}$ ; (b) the singular values of  $\mathbf{G}_1$ ; (c) the effective dimensionality against  $\beta$ ; (d) SNR<sub>1</sub> captured for the first target return against  $\beta$ ; (e) SNR<sub>2</sub> captured for the second target return against  $\beta$ .

for the bandpass modulated DPSS dictionary  $\mathbf{D}$  is chosen to be 30. We choose  $\beta = 10\%$ .

Figures 3(b-d) respectively display the target reconstruction result with 8 iterations of the subspace-based MP algorithm involving  $\Psi$ ,  $\bar{\Psi}$  and  $\hat{\Psi}$  (which means we use  $\Psi_{j_0}$ ,  $\bar{\Psi}_{j_0}$  and  $\hat{\Psi}_{j_0}$  respectively in Algorithm 1). We note that the wall clutter can be captured well by  $\hat{\mathbf{D}}$  and due to the limited space, we only show the region containing the targets in Figure 3. Clearly, we observe that the algorithm with  $\hat{\Psi}$  can find the second and the fifth targets which are very close to each other, while the algorithms with  $\Psi$  and  $\bar{\Psi}$  miss the fifth target.

As we have explained, the wall and target return subspaces have much smaller dimensionality when we consider them jointly across all antenna elements than separately for each antenna. This experiment demonstrates the advantage of using the joint target subspace in target detection.

TABLE I. THE LOCATION AND REFLECTIVITY OF THE TARGETS

$k$	1	2	3	4	5	6	7	8
$x$ (m)	-0.29	1.55	-1.69	-1.78	1.67	0.29	1	-1.3
$y$ (m)	5.38	6.38	6.58	4.93	5.03	6.6	4.97	3.63
$\sigma$	5	3	2	1	1	1	1	1

#### ACKNOWLEDGMENT

This work was supported by NSF grant CCF-1409261.

#### REFERENCES

- [1] M. Dehmollaian and K. Sarabandi, "Refocusing through building walls using synthetic aperture radar," *IEEE Trans. Geosci. Remote Sens.*, vol. 46, pp. 1589–1599, June 2008.
- [2] Y.-S. Yoon and M. Amin, "Spatial filtering for wall-clutter mitigation in through-the-wall radar imaging," *IEEE Trans. Geosci. Remote Sens.*, vol. 47, pp. 3192–3208, Sept 2009.
- [3] F. Tivive, A. Bouzerdoum, and M. Amin, "An SVD-based approach for mitigating wall reflections in through-the-wall radar imaging," in *Proc. 2011 IEEE Radar Conference*, pp. 519–524, May 2011.
- [4] E. Lagunas, M. Amin, F. Ahmad, and M. Najjar, "Joint wall mitigation and compressive sensing for indoor image reconstruction," *IEEE Trans. Geosci. Remote Sens.*, vol. 51, pp. 891–906, Feb 2013.
- [5] F. Ahmad, J. Qian, and M. Amin, "Wall clutter mitigation using Discrete Prolate Spheroidal Sequences for sparse reconstruction of indoor stationary scenes," *IEEE Trans. Geosci. Remote Sens.*, vol. 53, pp. 1549–1557, March 2015.
- [6] D. Slepian, "Prolate Spheroidal Wave Functions, Fourier analysis, and uncertainty—V: The discrete case," *Bell Syst. Tech. J.*, vol. 57, no. 5, pp. 1371–1430, 1978.
- [7] M. A. Davenport and M. B. Wakin, "Compressive sensing of analog signals using Discrete Prolate Spheroidal Sequences," *Appl. Comput. Harmon. Anal.*, vol. 33, no. 3, pp. 438–472, 2012.
- [8] Z. Zhu and M. B. Wakin, "Wall clutter mitigation and target detection using Discrete Prolate Spheroidal Sequences," in *3rd Int.*

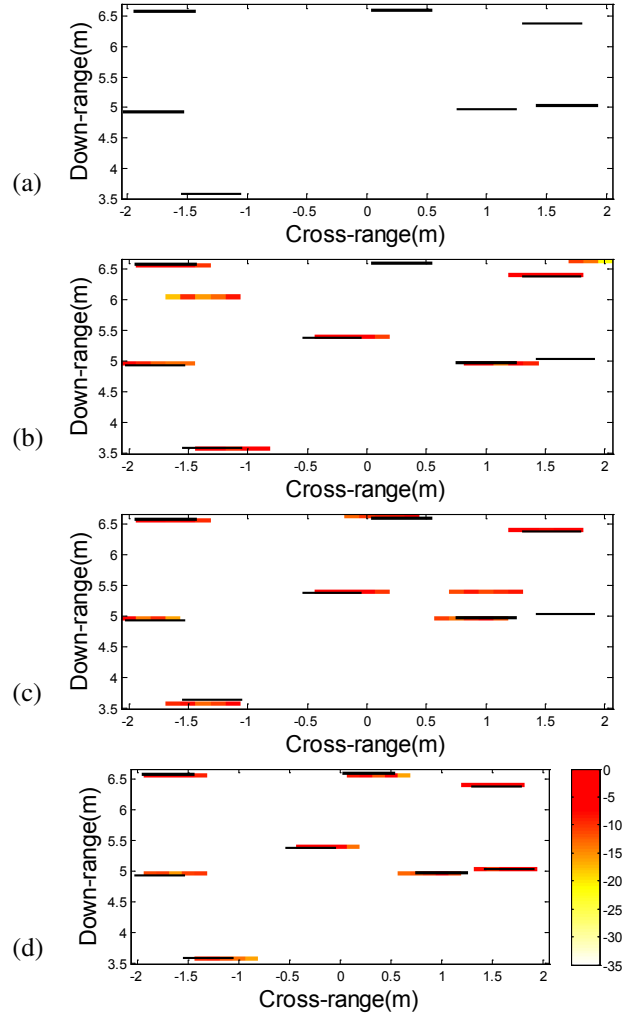


Fig. 3. Illustration of (a) the true target locations; and wall mitigation with  $\hat{\mathbf{D}}$  and target detection with subspace-based MP algorithm involving (b)  $\Psi$ ; (c)  $\bar{\Psi}$ ; (d)  $\hat{\Psi}$ .

*Workshop on Compressed Sensing Theory and its Applications to Radar, Sonar and Remote Sensing (CoSeRa)*, June 2015.

- [9] Z. Zhu and M. B. Wakin, "Detection of stationary targets using Discrete Prolate Spheroidal Sequences," in *31st International Review of Progress in Applied Computational Electromagnetics (ACES)*, pp. 1–2, March 2015.
- [10] E. Candès and M. Wakin, "An introduction to compressive sampling," *IEEE Signal Process. Mag.*, vol. 25, pp. 21–30, March 2008.
- [11] Z. Zhu and M. B. Wakin, "Approximating sampled sinusoids and multiband signals using multiband modulated DPSS dictionaries," to appear in *J. Fourier Anal. Appl.*, 2016.
- [12] S. G. Mallat and Z. Zhang, "Matching pursuits with time-frequency dictionaries," *IEEE Trans. Signal Process.*, vol. 41, no. 12, pp. 3397–3415, 1993.